

Atmospheric extinction coefficients in the Ic band for several major international observatories

Hale, Steven; Chaplin, William; Davies, Guy; Elsworth, Yvonne; Howe, Rachel; Lund, Mikkel; Moxon, E; Thomas, A; Pallé, P. L.; Rhodes, Ed

DOI:

[10.3847/1538-3881/aa81d0](https://doi.org/10.3847/1538-3881/aa81d0)

Document Version

Peer reviewed version

Citation for published version (Harvard):

Hale, S, Chaplin, W, Davies, G, Elsworth, Y, Howe, R, Lund, M, Moxon, E, Thomas, A, Pallé, PL & Rhodes, E 2017, 'Atmospheric extinction coefficients in the Ic band for several major international observatories: Results from the BiSON telescopes, 1984 to 2016', *The Astronomical Journal*, vol. 154, no. 89.
<https://doi.org/10.3847/1538-3881/aa81d0>

[Link to publication on Research at Birmingham portal](#)

General rights

Unless a licence is specified above, all rights (including copyright and moral rights) in this document are retained by the authors and/or the copyright holders. The express permission of the copyright holder must be obtained for any use of this material other than for purposes permitted by law.

- Users may freely distribute the URL that is used to identify this publication.
- Users may download and/or print one copy of the publication from the University of Birmingham research portal for the purpose of private study or non-commercial research.
- User may use extracts from the document in line with the concept of 'fair dealing' under the Copyright, Designs and Patents Act 1988 (?)
- Users may not further distribute the material nor use it for the purposes of commercial gain.

Where a licence is displayed above, please note the terms and conditions of the licence govern your use of this document.

When citing, please reference the published version.

Take down policy

While the University of Birmingham exercises care and attention in making items available there are rare occasions when an item has been uploaded in error or has been deemed to be commercially or otherwise sensitive.

If you believe that this is the case for this document, please contact UBIRA@lists.bham.ac.uk providing details and we will remove access to the work immediately and investigate.

ATMOSPHERIC EXTINCTION COEFFICIENTS IN THE I_c BAND FOR SEVERAL MAJOR
INTERNATIONAL OBSERVATORIES:
RESULTS FROM THE BISON TELESCOPES, 1984 TO 2016

S. J. HALE,^{1,2} W. J. CHAPLIN,^{1,2} G. R. DAVIES,^{1,2} Y. P. ELSWORTH,^{1,2} R. HOWE,^{1,2} M. N. LUND,^{1,2}
E. Z. MOXON,^{1,2} A. THOMAS,^{1,2} P. L. PALLÉ,³ AND E. J. RHODES, JR.^{4,5}

¹*School of Physics and Astronomy, University of Birmingham, Edgbaston, Birmingham B15 2TT, United Kingdom*

²*Stellar Astrophysics Centre, Department of Physics and Astronomy, Aarhus University, Ny Munkegade 120, DK-8000 Aarhus C, Denmark*

³*Instituto de Astrofísica de Canarias, and Department of Astrophysics, Universidad de La Laguna, San Cristóbal de La Laguna, Tenerife, Spain*

⁴*Department of Physics and Astronomy, University of Southern California, Los Angeles, CA 90089, USA*

⁵*Astrophysics and Space Sciences Section, Jet Propulsion Laboratory California Institute of Technology, 4800 Oak Grove Dr., Pasadena, CA 91109-8099, USA*

(Received May 9, 2017; Revised July 3, 2017; Accepted July 20, 2017)

Submitted to AJ

ABSTRACT

Over 30 years of solar data have been acquired by the Birmingham Solar Oscillations Network (BiSON), an international network of telescopes used to study oscillations of the Sun. Five of the six BiSON telescopes are located at major observatories. The observational sites are, in order of increasing longitude: Mount Wilson (Hale) Observatory (MWO), California, USA; Las Campanas Observatory (LCO), Chile; Observatorio del Teide, Izaña, Tenerife, Canary Islands; the South African Astronomical Observatory (SAAO), Sutherland, South Africa; Carnarvon, Western Australia; and the Paul Wild Observatory, Narrabri, New South Wales, Australia. The BiSON data may be used to measure atmospheric extinction coefficients in the I_c band (approximately 700 nm to 900 nm), and presented here are the derived atmospheric extinction coefficients from each site over the years 1984 to 2016.

Keywords: atmospheric effects — Sun: helioseismology — Sun: oscillations

arXiv:1707.06647v1 [astro-ph.IM] 20 Jul 2017

1. INTRODUCTION

The *Birmingham Solar Oscillations Network* (BiSON) is a six-site ground-based network of solar observatories. The primary science output of the network is detection of solar oscillations. Here, we take an alternative window into these data and assess the historic atmospheric column extinction coefficients at each of our international network sites, over the life of the network. The history and performance of the network is detailed in Hale et al. (2016). In summary, the first instrument was commissioned at Observatorio del Teide in Izaña, Tenerife, in 1975, with the additional five nodes coming online throughout the mid-80s and early-90s. The observational sites are, in order of increasing longitude: Mount Wilson (Hale) Observatory (MWO), California, USA; Las Campanas Observatory (LCO), Chile; Observatorio del Teide, Izaña, Tenerife, Canary Islands; South African Astronomical Observatory (SAAO), Sutherland, South Africa; Carnarvon, Western Australia; Paul Wild Observatory, Narrabri, New South Wales, Australia. The network operates continuously and provides an annual data duty cycle averaging around 82%. The locations of the network nodes are summarised in Table 1.

In the next section we will take a brief look at the network instrumentation and in section 3 describe how the atmospheric-extinction coefficients are determined. We will then go on to present the historic extinction coefficients of each site in section 4.

2. INSTRUMENTATION

The BiSON solar spectrometers provide very precise measures of the disc-averaged line-of-sight velocity of the solar surface. This is done by comparing the wavelength of the potassium absorption line at 769.898 nm formed within the Sun, with the same line in a vapor reference cell on Earth. The spectrometers typically have three photo-detectors. Two of the detectors measure the intensity of the light scattered from the vapor cell, and the third measures the intensity of light transmitted directly through the instrument. The light is pre-filtered using an I_c band filter (approximately 700 nm to 900 nm) formed from Schott RG9 and KG4 glass, and the bandwidth is then reduced again to 15 Å using an interference filter centred on 769.9 nm. The width of the potassium absorption line is significantly narrower than 15 Å, and so the measurement of the transmitted light can be considered to be a measurement of the direct-Sun radiance near the center of the I_c band – essentially the instrument becomes an automated solar photometer. Where a measurement of the transmitted light is not available, the light scattered from the vapor cell can also be used as a proxy for the transmitted intensity – see the ap-

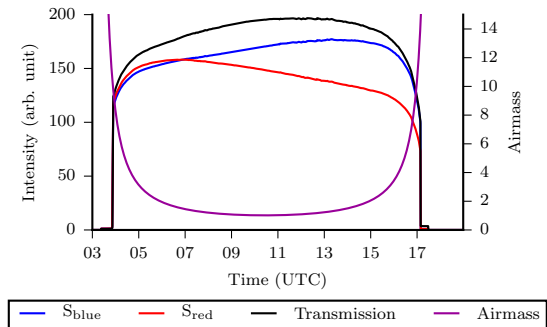


Figure 1. Data from 2014 December 1 at Sutherland, South Africa. The black line shows the transmitted solar intensity. The blue and red lines show respectively the measured intensity at points on the shorter-wavelength (S_{blue}) and longer-wavelength (S_{red}) ‘wings’ of the potassium absorption line at 769.898 nm. The variation in airmass is shown by the magenta line, measured against the right-axis.

pendix for further details. Figure 1 shows a typical day of data captured from the site at Sutherland, along with the variation in airmass during the day. The data have been pre-processed to remove any periods of instrumental failure and cloudy conditions. Even thin cirrus produces an easily identifiable reduction in data quality, and so the data analysed in this paper are from clear sky observations only.

3. DERIVING EXTINCTION COEFFICIENTS

Atmospheric extinction has three main components: Rayleigh scattering, scattering due to aerosols, and molecular absorption. The strongest absorption effects are due to molecular oxygen and ozone which both absorb in the ultraviolet, and water vapor which absorbs in the infrared. At the BiSON observational wavelength of 769.9 nm, Rayleigh scattering is at a level of a few percent, and there is no molecular absorption: the observed atmospheric extinction is dominated by the contribution of aerosols.

The Beer-Lambert law states that the transmittance, T , of a material is related to its optical depth, τ_λ , by

$$T = \frac{I}{I_0} = e^{-\tau_\lambda A} , \quad (1)$$

where I_0 is the solar extraterrestrial radiance (i.e., at zero airmass), and I is the direct-Sun radiance. In this case τ_λ is the column atmospheric aerosol optical depth (AOD) per unit airmass, and A is the relative optical airmass as a function of solar zenith angle. The aerosol optical depth is typically quoted as unitless when considering only the unit airmass at the zenith. By taking the natural logarithm of both sides we obtain,

$$\ln(I/I_0) = -\tau_\lambda A , \quad (2)$$

Table 1. Coordinates of the six-station Birmingham Solar Oscillations Network (BiSON)

Location	Longitude [deg E]	Latitude [deg N]	Altitude [m]	Commissioned [year]
Mount Wilson, California, USA	-118.08	+34.13	1742	1992
Las Campanas, Chile	-70.70	-29.02	2282	1991
Izaña, Tenerife, Canary Islands	-16.50	+28.30	2368	1975
Sutherland, South Africa	+20.82	-32.38	1771	1990
Carnarvon, Western Australia	+113.75	-24.85	10	1985
Narrabri, New South Wales, Australia	+149.57	-30.32	217	1992

which gives a convenient linear relationship where the gradient of the relationship is a measure of τ_λ , and I_0 is now simply a normalization factor taken as the maximum intensity measured on a given day. For astronomical use, we rescale AOD in terms of magnitude,

$$\begin{aligned} \kappa_\lambda &= -2.5 \log_{10}(e)(-\tau_\lambda) , \\ &= 1.086\tau_\lambda , \end{aligned} \quad (3)$$

where κ_λ is the atmospheric extinction coefficient, with units of magnitudes per airmass. More accurately, this is the column extinction coefficient since we do not include any knowledge on the vertical structure of the atmosphere. Readers in the climate modeling and aerosol communities should divide the values presented here by 1.086 in order to recover the total column-aerosol in terms of aerosol optical depth (AOD).

In this analysis, the known zenith-angle was used to calculate the airmass based on [Kasten & Young \(1989\)](#) who define the airmass as,

$$A = \frac{1}{\cos z + 0.50572(6.07995 + 90 - z)^{-1.6364}} , \quad (4)$$

where the zenith-angle z is in degrees. This model gives an airmass of approximately 38 at the horizon, producing good results for the whole range of zenith-angles.

The extinction coefficients were determined using two methods: Firstly by making a standard linear least-squares fit of the magnitude-like value from equation 2 against airmass, and secondly by calculating the non-overlapping independent first-differences and then obtaining statistical estimations from the histogram of a timeseries of,

$$\frac{dm}{dA} = \frac{m_i - m_{i-1}}{A_i - A_{i-1}} , \quad (5)$$

where m is the magnitude-like value from equation 2, A is airmass, and i is the sample index incremented in steps

of two. In our fits we consider only air masses in the range of 2 to 5, corresponding to zenith-angles between approximately 60° to 80° , since this is the region where airmass is changing most linearly. Below two air-masses the change does not follow a strictly linear relationship and is not well described by a straight line fit. The rate-of-change is also too low to allow good fitting. Additionally, we need to ensure we remove the seasonal variations in minimum air-mass due to the changing maximum altitude of the Sun throughout the year, since this could introduce an artificial seasonal effect in the derived extinction values. Above five air-masses the rate of change is too high, producing differential extinction across the extended source of the Sun ([Davies et al. 2014](#)). The pre-meridian and post-meridian values (hereafter referred to as ‘morning’ and ‘afternoon’) are fitted separately, since it is expected that these will differ due to local environmental considerations. The results from both techniques for the same day as in Figure 1 are shown in Figure 2.

The coefficient estimation technique and the selection of airmass range-limits affects the value of the determined extinction. In order to investigate the robustness of our parameters, a randomization trial was performed where rather than fixing the lower and upper airmass limits at 2 and 5 respectively, they were randomly selected each day between 2–3 and 4–5 air-masses. Five realisations were then generated for the full timeseries of fitted extinction gradients from each site, and the absolute difference was compared between each realisation and the gradients measured when the airmass limits were fixed. A similar comparison was made between the timeseries of fitted gradients, and a timeseries of median first-differences. In all cases, the mean difference was less than 4% of the mean extinction. The standard deviation of the difference was 3 to 6 times lower than the measured extinction standard deviation. Any systematic offsets or increase in scattering due to the processing techniques are at a level significantly lower

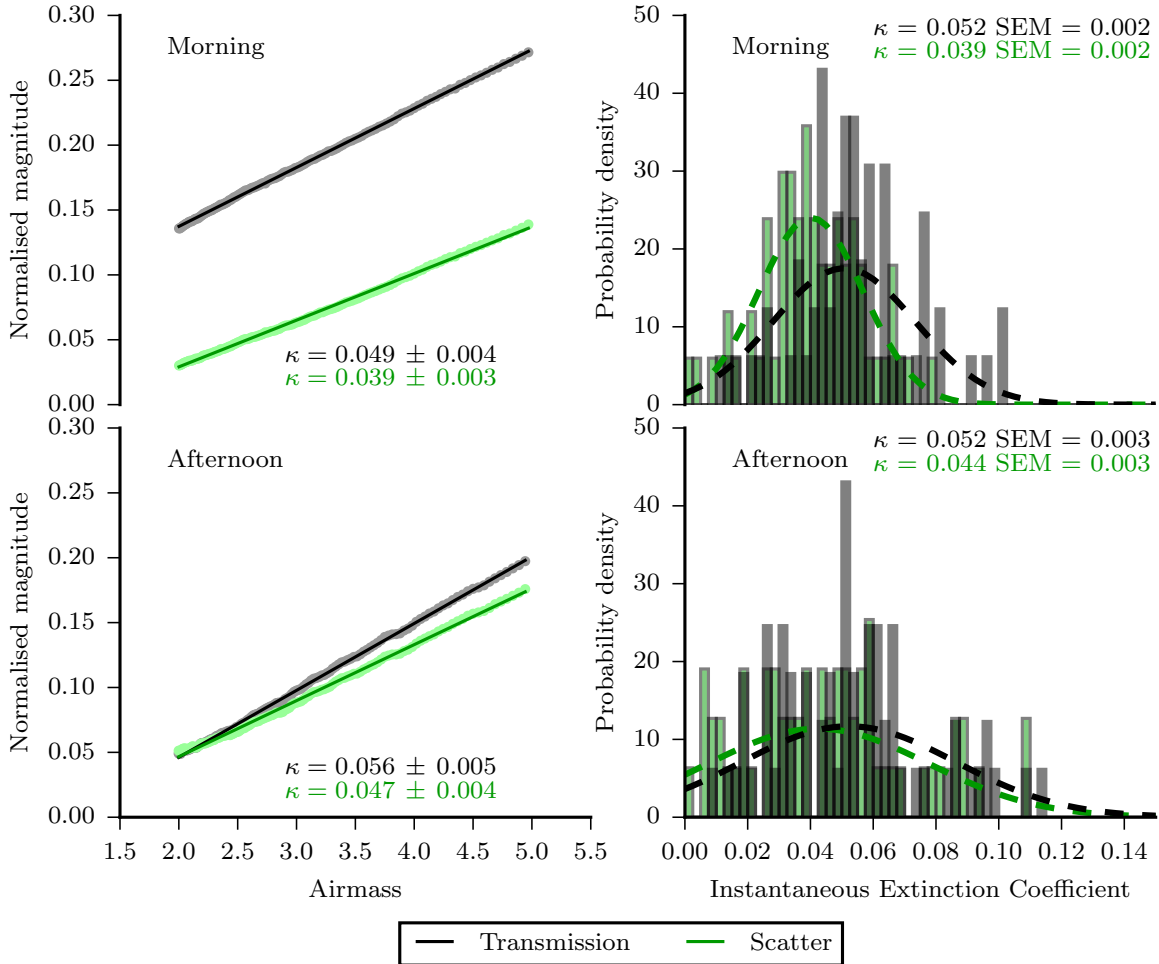


Figure 2. Morning and afternoon extinction coefficients for 2014 December 1 at Sutherland, South Africa. The values determined are shown in the plot. Left column: The formal uncertainty on the fit is calculated from the covariance matrix returned by the fitting function. Right column: The uncertainty on the histogram is the standard-error of the median (SEM), i.e., 0.741 times the interquartile range of the distribution divided by the square-root of the number of points. The dashed lines on the histograms represent for comparison the equivalent Gaussian profile for the measured mean and standard deviation.

than that due to real physical effects. These two techniques are considered to be equivalent, and the results presented here are produced solely from the first method using linear least-squares fitting.

In the next section we present fitted extinction coefficients for all the historic data from each BiSON site. For clarity the units of extinction will no longer be stated on each value in the text. All extinction values are specified in magnitudes per airmass. During the discussion for each site, we quote either mean, mode, or median values depending on the values required for comparisons with other studies. For consistency, a summary of the coefficients is given in Table 2. Since there are significant seasonal differences, we also present the values measured over two months for each mid-summer (July-August in the northern hemisphere, January-February in the southern hemisphere) in Table 3, and during mid-

winter (January-February in the northern hemisphere, July-August in the southern hemisphere) in Table 4.

4. SITES

4.1. Izaña, Tenerife

The BiSON node at Tenerife (Roca Cortés & Pallé 2014) is based at the Observatorio del Teide, which is operated by the IAC (*Instituto de Astrofísica de Canarias*). The Canary Islands are located about 100 km to the west of the North African coast. The islands are close to the Western Sahara and so during the summer months they frequently experience high concentrations of mineral dust in the atmosphere. This aerosol concentration is easily seen in Figure 3 as the strong seasonal variation in extinction.

The modal values of the extinction distributions are 0.054 in the morning and 0.046 in the afternoon

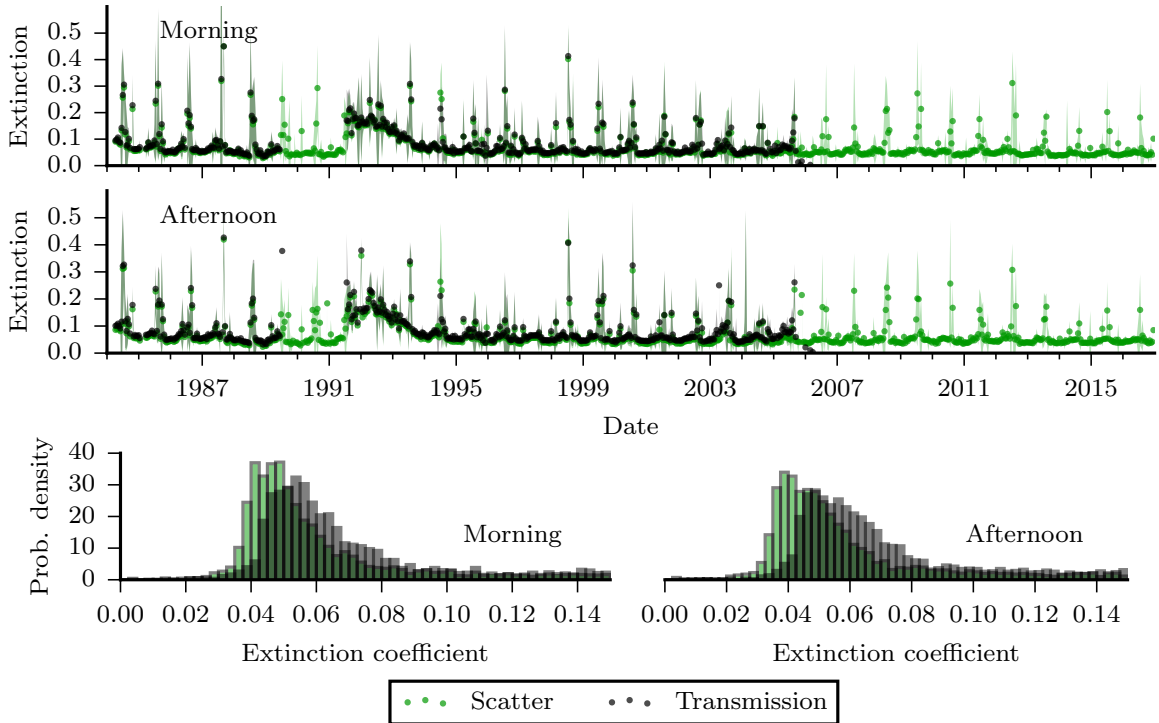


Figure 3. Extinction coefficients and statistical distribution from Izaña, Tenerife. Each dot represents the median value over 14 days. The coloured banding represents ± 3 times the standard-error on each median. Dates indicate January 1 for each year.

for transmission. The standard deviation on these values is 0.09, the high value being indicative of the large scatter in values between summer and winter periods. The difference in the values pre-meridian and post-meridian is likely due to the surrounding geography, where morning extinction effects are through atmosphere over North Africa and afternoon is over the potentially clearer North Atlantic ocean. If only the winter months are considered, then the modal value for both morning and afternoon drops to 0.045 with correspondingly reduced scatter. Mineral dust events are typical between June and October, where extinction values anywhere from 0.1 to 0.8 may be experienced. The extinction values derived from the scattered-light are a slight underestimate as expected (see appendix), but otherwise show the same trends. The distribution of extinction coefficients appears to show two combined trends, the first a set of normally-distributed values centred on approximately 0.05, and a long positive tail that corresponds to the periods of mineral dust events. If the summer and winter periods are analysed separately, then the winter does indeed show a mean of approximately 0.05 to 0.06, and the summer a much higher mean of 0.14 to 0.15 with correspondingly higher standard deviation. A similar atmospheric analysis on data from telescopes on the Canary Archipelago, which included our BiSON data from this instrument, was

made by [Laken et al. \(2016\)](#) and the modal values are consistent given the uncertainties. [Laken et al. \(2016\)](#) provides a thorough investigation into the occurrence of dust events, and how they change over both short seasonal periods and longer time scales. Several authors have investigated this in more detail {see, e.g., [Guerrero et al. \(1998\)](#); [Jimenez et al. \(1998\)](#); [Siher et al. \(2004\)](#); [García-Gil et al. \(2010\)](#); [Laken et al. \(2014\)](#)}.

[Siher et al. \(2002\)](#) present extinction values for the IRIS (*International Research of the Interior of the Sun*) site based at Izaña. IRIS was a similar network to BiSON and used a similar observational technique but made use of the shorter wavelength sodium absorption line at 589.6 nm. They quote an average extinction value of 0.111, which is slightly higher than the mean values found here. The higher value is expected due to their use of the shorter wavelength, since shorter wavelengths tend to suffer greater extinction. [Jimenez et al. \(1998\)](#) found the extinction to vary during 1984 to 1989 between 0.04 to 0.07 at 680 nm, which is in agreement with the values found here for Izaña. During dust storms [Jimenez et al. \(1998\)](#) reported values up to 0.8, which again is in agreement with our findings. The GONG (*Global Oscillation Network Group*) site-survey ([Hill et al. 1994](#)) at Izaña measured an average extinction value of 0.1169 from 1985 September to 1993 July. GONG is another network similar to Bi-

SON. Their initial site-survey used a normal incidence pyrhelimeter (NIP) manufactured by Eppley Laboratories (Fischer et al. 1986) which has a wide spectral sensitivity range of 250 nm to 3000 nm. Light from the Sun is broadly like that of a black body at a temperature of 6000 K, meaning that the intensity peaks at a wavelength of approximately 500 nm and decays quickly in the infrared. The value measured by the pyrhelimeter will be strongly weighted towards the peak wavelength of the solar spectrum. King (1985) discusses the wavelength dependence of typical expected atmospheric extinction from 300 nm to 1100 nm at the Roque de los Muchachos Observatory, on the adjacent island of La Palma. At 500 nm an extinction coefficient of 0.1244 can be expected, very close to the value determined during the GONG site-survey. At 300 nm, near the short end of the pyrhelimeter sensitivity range, values well over 3 can be expected. The average extinction measured by the pyrhelimeter will be much higher than the monochromatic values measured by BiSON at 769.9 nm, and unfortunately this means that no comparison can be made between the results from BiSON and the GONG site-survey.

Probably the most striking feature in Figure 3 is the increase in extinction following the eruption of Mount Pinatubo in the Philippines on 1991 June 15. There is also a hint of the tail-end of effects from the El Chichón eruption in Mexico in 1982 April where the start of the data in 1984 show extinction values around 0.1, double the typical value expected outside of a dust intrusion. Both Guerrero et al. (1998) and García-Gil et al. (2010) have previously observed these features from telescopes based at the Canary Islands.

4.2. Carnarvon

The BiSON node at Carnarvon is based at the historic *Overseas Telecommunications Commission Satellite Earth Station*, around 900 km north of Perth in Western Australia. The measured extinction coefficients over the operational lifetime of the site are shown in Figure 4.

The median morning extinction is 0.072, and the afternoon is 0.078. This increases to approximately 0.1 in the summer and decreases to around 0.06 in the winter. The standard deviation shows a similar increase in summer compared to winter. In the summer the standard deviation is noticeably lower in the afternoon compared to the morning, at 0.05 and 0.07 respectively. Morning data are collected over the plains of Western Australia, and afternoon data are through air over the Indian ocean, and so it is expected that the sandy environment of Carnarvon would have greater impact on

extinction during morning observations. There are no comparison sites available near Carnarvon.

4.3. Sutherland

The BiSON node at Sutherland is situated 360 km north-east of Cape Town, at the *South African Astronomical Observatory* (SAAO). The measured extinction coefficients over the operational lifetime of the site are shown in Figure 5.

The median morning extinction is 0.046, and afternoon is 0.045. There are no significant differences in environment around Sutherland, and this is reflected by the stability of the extinction coefficients between morning and afternoon. The site shows stable performance with little change in the median values throughout a year. The atmosphere is particularly stable, with standard deviations of between 0.04 and 0.06 in the winter, and approximately 0.02 during the summer. Kilkeny (1995) state a mean extinction coefficient of 0.07 in the I_c band which is slightly higher than found here, but is within our measured standard deviation.

4.4. Las Campanas

The BiSON node at Las Campanas is situated 630 km north of Santiago, at the *Las Campanas Observatory*. The measured extinction coefficients over the operational lifetime of the site are shown in Figure 6.

Transmission data from this site are unreliable due to instrumentation issues, and so only the scattered-light data have been used to derive the extinction coefficients. The median extinction is 0.033 for both morning and afternoon, with standard deviation of less than 0.02. There is also little variation between winter and summer periods with mean extinction at 0.028 and 0.042 respectively. Morning data are collected through airmasses over South America, and afternoon data are through air over the South Pacific ocean. There appears to be no significant difference between the two zones, and Las Campanas has the most stable atmosphere of all BiSON sites, showing the lowest standard deviation.

Siher et al. (2002) performed a similar atmospheric analysis for the IRIS site based at La Silla, the adjacent mountain ridge to Las Campanas. They quote a value of 0.097, which is higher than found here, but we again have to consider the shorter wavelength used by IRIS, and also that we expect the extinction from the scattered light to be a slight underestimate of the equivalent extinction from the transmitted light. The measured standard deviation is similar at 0.028.

4.5. Narrabri

The BiSON node at Narrabri is situated 525 km north-west of Sydney, at the *Paul Wild Observatory*. The mea-

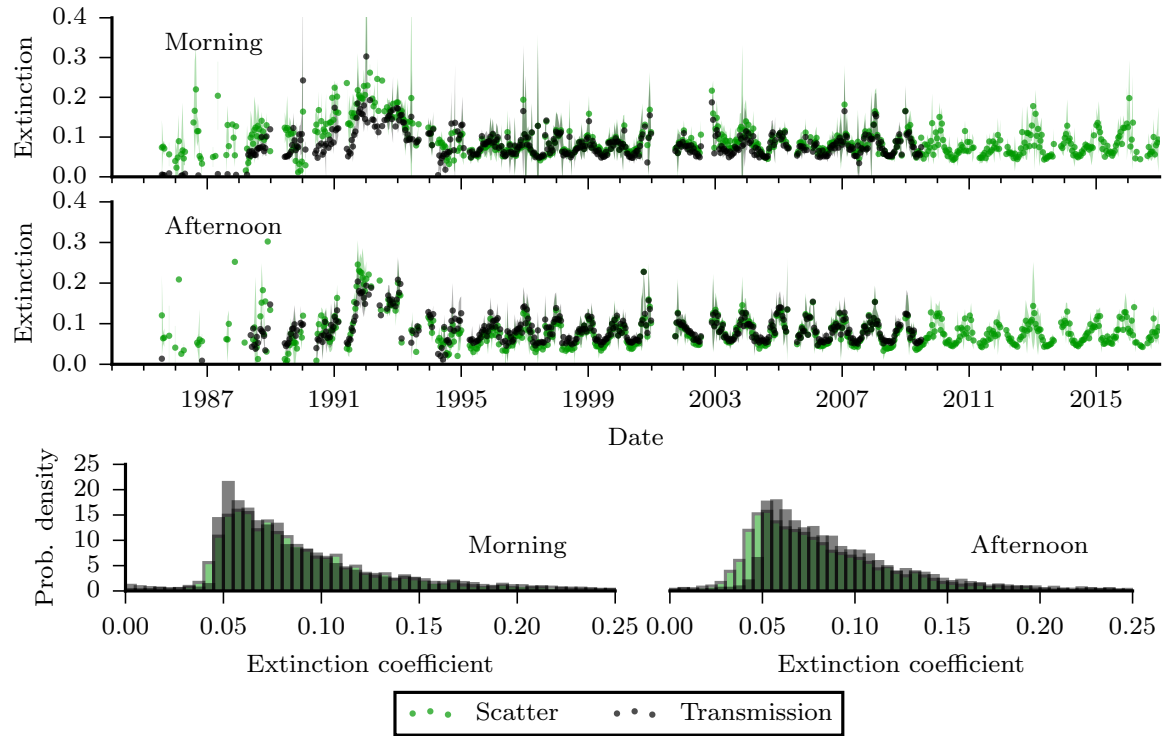


Figure 4. Extinction coefficients and statistical distribution from Carnarvon, Western Australia. Each dot represents the median value over 14 days. The coloured banding represents ± 3 times the standard-error on each median. Dates indicate January 1 for each year.

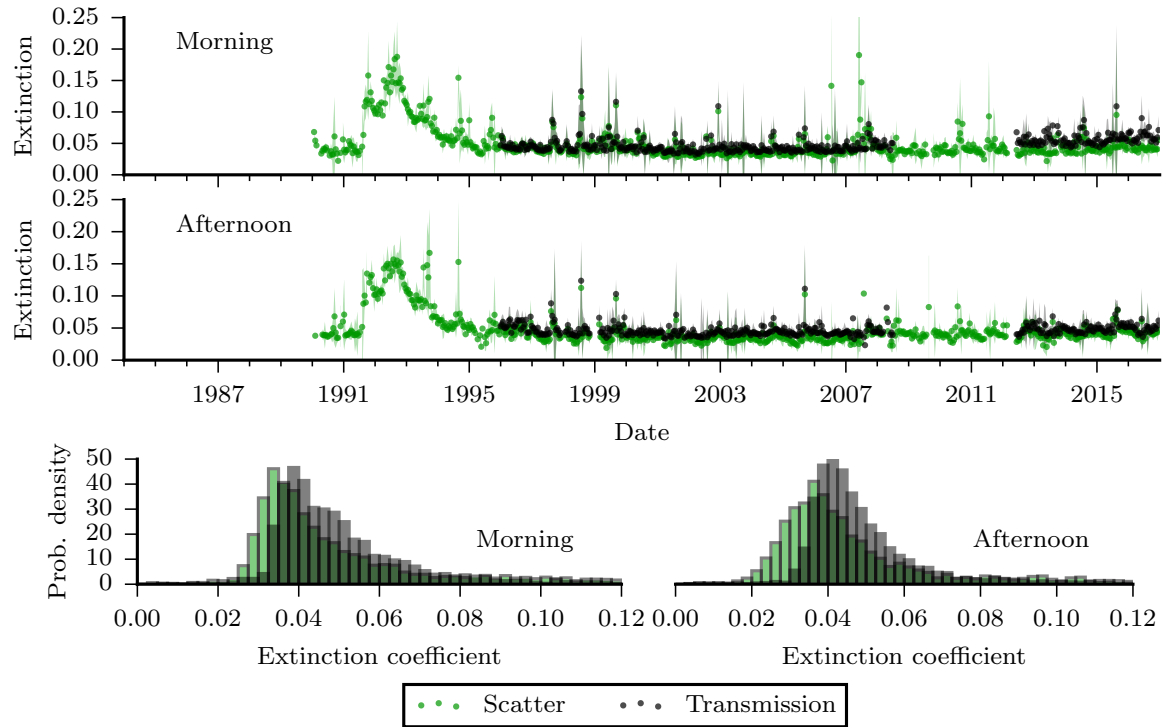


Figure 5. Extinction coefficients and statistical distribution from Sutherland, South Africa. Each dot represents the median value over 14 days. The coloured banding represents ± 3 times the standard-error on each median. Dates indicate January 1 for each year.

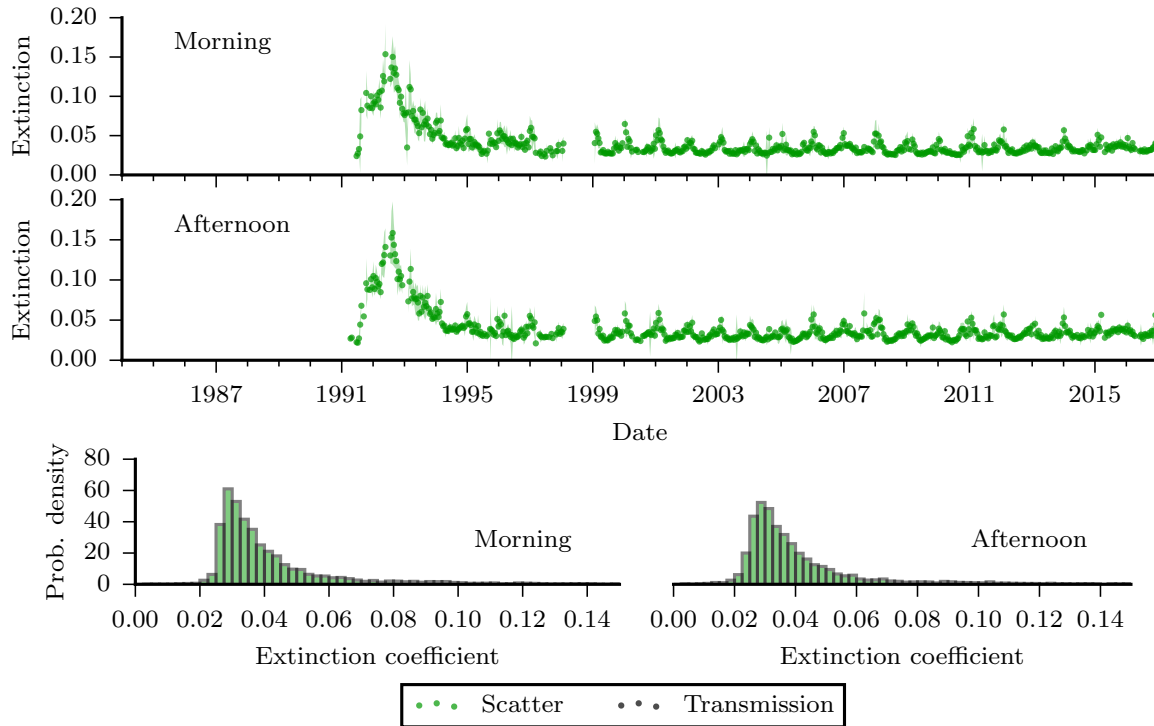


Figure 6. Extinction coefficients and statistical distribution from Las Campanas, Chile. Each dot represents the median value over 14 days. The coloured banding represents ± 3 times the standard-error on each median. Dates indicate January 1 for each year. There is no transmitted-light measured at Las Campanas, and so only the scattering values are presented.

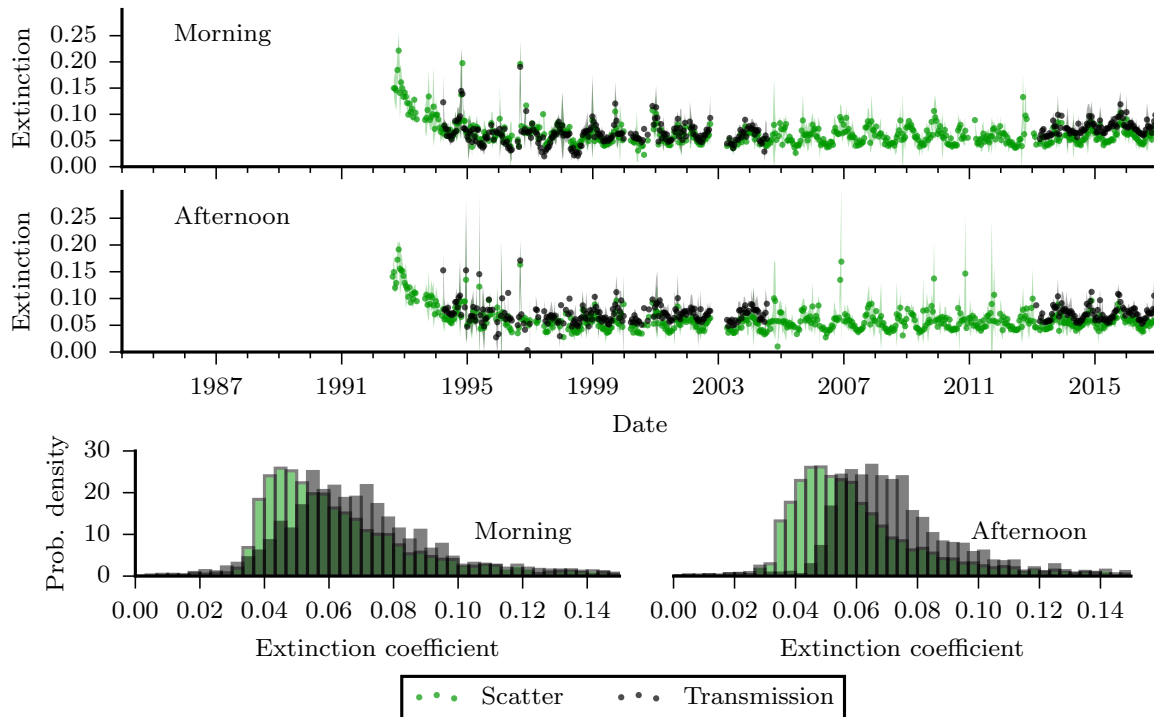


Figure 7. Extinction coefficients and statistical distribution from Narrabri, eastern Australia. Each dot represents the median value over 14 days. The coloured banding represents ± 3 times the standard-error on each median. Dates indicate January 1 for each year.

sured extinction coefficients over the operational lifetime of the site are shown in Figure 7.

The median morning extinction is 0.074, and afternoon is 0.077. The standard deviation is approximately 0.04. There are no significant differences in environment around Narrabri and again this is reflected in the stability of the extinction coefficients between morning and afternoon. There is, however, a strong seasonal variation with median values dropping to 0.06 in the winter and rising to almost 0.08 in the summer. Narrabri tends to have lower extinction and lower standard deviation than the coastal town of Carnarvon, although it does suffer from a higher percentage of cloudy days overall. No datasets could be found for comparison with Narrabri.

4.6. Mount Wilson

The BiSON node at Mount Wilson is situated 52 km north-east of Los Angeles, at the *Mount Wilson (Hale) Observatory*. The measured extinction coefficients over the operational lifetime of the site are shown in Figure 8.

The median morning extinction is 0.085, and afternoon is 0.081. Mount Wilson is an atmospherically-interesting site due to its location close to the major city of Los Angeles. Morning data are collected over the San Gabriel mountains, while afternoon data are observed through air over the city, and so it may be expected that afternoon extinction values would be worse. The median-values found here show that morning and afternoon are generally similar, however the modal values do show an increase from 0.048 in the morning to 0.070 in the afternoon. There is an upward trend in extinction levels from around 1999, becoming from 2007 part of the large scatter in values that could be considered to be a result of the highly variable atmosphere near a large city. In clear sky conditions during our observations the inversion boundary layer traps any pollution at a relatively low altitude — the well-known Los Angeles smog. Since the observatory elevation is well above the inversion layer, the pollution would not be seen except at very high zenith angles that have been specifically excluded from this analysis. At this site, light is collected via two mirrors, known as a coelostat, and it is possible that the increase in scatter is due to gradual reduction in performance due to deterioration of the mirrors; however, since the extinction is determined from a daily calibration, any variation in long term performance is removed completely and so this is just speculation and the cause of the increased scatter is not clear. During the winter months, Mount Wilson does suffer a high proportion of cloudy days, but when the sky is clear there appears to be little variation be-

tween seasons, both in terms of absolute extinction and standard deviation.

4.7. Site summary

A summary of the extinction coefficients from 1995 over all seasons is given in Table 2. In order to compare seasonal differences, the values measured over two months for each mid-summer (July-August in the northern hemisphere, January-February in the southern hemisphere) are presented in Table 3, and during mid-winter (January-February in the northern hemisphere, July-August in the southern hemisphere) in Table 4.

5. CONCLUSION

Over 30 years of helioseismic data have been acquired by BiSON from several international observatories, the locations of which are summarised in Table 1. In this paper we have made innovative use of these data to derive measurements of atmospheric opacity in the I_c band, and we have presented the column atmospheric extinction coefficients from each site over the years 1984 to 2016. This is an important contribution to the literature since there are limited data on aerosol optical depth from other sources prior to the mid-1990s.

The median and standard deviation values for mid-summer periods from Table 3, and for mid-winter periods from Table 4, are shown graphically in Figure 9. The mean of the morning and afternoon values were taken for each site, and the extinction distribution standard deviation shown as error bars. We find the best results are from the Las Campanas and Sutherland observatories with consistent year-round performance. Izaña offers comparable high-performance during the winter months, but becomes the worst site during mid-summer due to high concentrations of mineral dust in the atmosphere from the Western Sahara on the North African coast. Carnarvon similarly suffers degradation during the summer months, which again is most likely due to wind-borne sand in the dry environment of northern Western Australia. Narrabri and Mount Wilson both offer consistent performance.

The atmospheric extinction data presented here and the code to generate the figures are open access and can be downloaded from the University of Birmingham ePapers data archive (Hale 2017).

We would like to thank all those who have been associated with BiSON over the years. We particularly acknowledge the technical assistance at our remote network sites, with sincere apologies to anyone inadvertently missed: In Mount Wilson: Stephen Pinkerton, the team of USC undergraduate observing assistants,

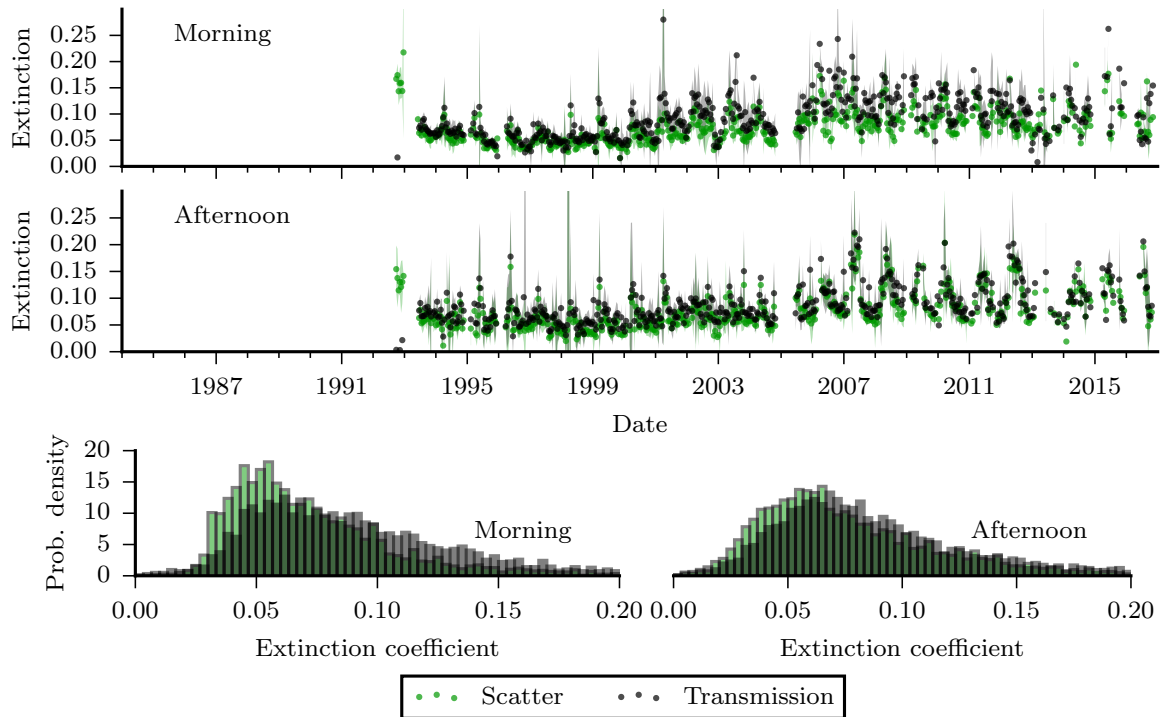


Figure 8. Extinction coefficients and statistical distribution from Mount Wilson, California USA. Each dot represents the median value over 14 days. The coloured banding represents ± 3 times the standard-error on each median. Dates indicate January 1 for each year.

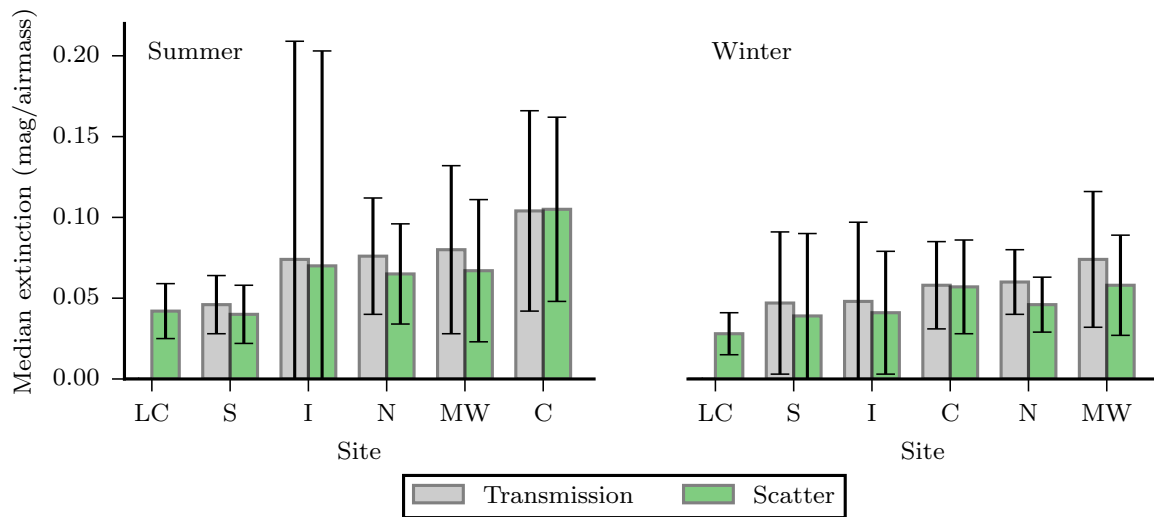


Figure 9. Summary of median extinction coefficients and distribution standard deviations. Only 1995 onwards has been considered in order to remove any exceptional atmospheric events. Left panel: Summer periods from Table 3. Right panel: Winter periods from Table 4. The mean of the morning and afternoon median coefficients have been taken for each site, and the extinction distribution standard deviation shown as error bars. The x-axis labels are the initials of each site name.

Table 2. Extinction coefficients from all sites. Only 1995 onwards has been considered in order to remove any exceptional atmospheric events. The data-sets are sufficiently large that the standard error of the mean (i.e., σ/\sqrt{N}) is very small and therefore not presented.

Location	Detector	Mode	Median	Mean	Sigma
Mount Wilson	Transmission (Morning)	0.048	0.085	0.096	0.055
Mount Wilson	Transmission (Afternoon)	0.070	0.081	0.093	0.057
Mount Wilson	Scatter (Morning)	0.056	0.064	0.074	0.043
Mount Wilson	Scatter (Afternoon)	0.061	0.070	0.082	0.053
Las Campanas	Transmission (Morning)				
Las Campanas	Transmission (Afternoon)				
Las Campanas	Scatter (Morning)	0.029	0.033	0.037	0.018
Las Campanas	Scatter (Afternoon)	0.028	0.033	0.036	0.014
Izaña	Transmission (Morning)	0.054	0.058	0.092	0.090
Izaña	Transmission (Afternoon)	0.046	0.060	0.092	0.091
Izaña	Scatter (Morning)	0.048	0.051	0.082	0.084
Izaña	Scatter (Afternoon)	0.039	0.049	0.079	0.087
Sutherland	Transmission (Morning)	0.038	0.046	0.054	0.040
Sutherland	Transmission (Afternoon)	0.039	0.045	0.051	0.026
Sutherland	Scatter (Morning)	0.034	0.039	0.048	0.039
Sutherland	Scatter (Afternoon)	0.037	0.038	0.044	0.027
Carnarvon	Transmission (Morning)	0.052	0.072	0.085	0.050
Carnarvon	Transmission (Afternoon)	0.052	0.078	0.088	0.043
Carnarvon	Scatter (Morning)	0.057	0.074	0.087	0.049
Carnarvon	Scatter (Afternoon)	0.052	0.071	0.081	0.043
Narrabri	Transmission (Morning)	0.053	0.066	0.070	0.029
Narrabri	Transmission (Afternoon)	0.061	0.068	0.073	0.025
Narrabri	Scatter (Morning)	0.048	0.055	0.062	0.028
Narrabri	Scatter (Afternoon)	0.050	0.053	0.059	0.027

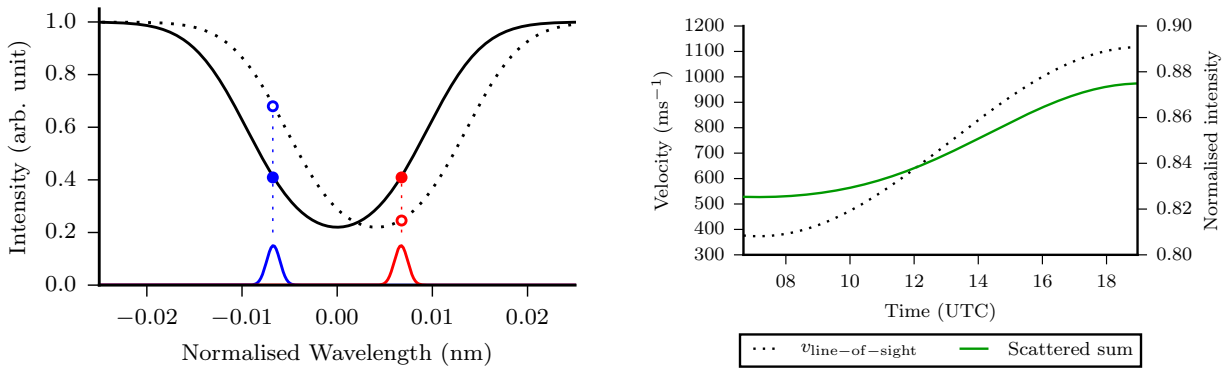


Figure 10. Left: The solid line represents an absorption line with zero line-of-sight velocity offset. The sum of the intensity measurement of the two wings (solid circles) is 0.82. The dashed line represents an offset where $v_{\text{line-of-sight}}$ is 1600 ms^{-1} . The sum of the intensity measurement of the two wings (open circles) rises to 0.93. Neither measurement returns the unity intensity measured outside the absorption line. Right: The expected variation in scattered-sum over typical line-of-sight Doppler velocities, in the absence of any atmospheric extinction. The amplitude of the daily change in effective-intensity varies throughout the year with changes in Earth’s orbital velocity.

former USC staff members Maynard Clark, Perry Rose, Natasha Johnson, Steve Padilla, and Shawn Irish, and former UCLA staff members Larry Webster and John Boyden. In Las Campanas: Patricio Pinto, Andres Fuentevilla, Emilio Cerda, Frank Perez, Marc Hellebaut, Patricio Jones, Gastón Gutierrez, Juan Navarro, Francesco Di Mille, Roberto Bermudez, and the staff of LCO. In Izaña: All staff at the IAC who have contributed to running the Mark I instrument over many years. In Sutherland: Pieter Fourie, Willie Koorts, Jaci Cloete, Reginald Klein, John Stoffels, and the staff

of SAAO. In Carnarvon: Les Bateman, Les Schultz, Sabrina Dowling-Giudici, Inge Lauw of Williams and Hughes Lawyers, and NBN Co. Ltd. In Narrabri: Mike Hill and the staff of CSIRO. MNL acknowledges the support of The Danish Council for Independent Research | Natural Sciences (Grant DFF-4181-00415). Funding for the Stellar Astrophysics Centre (SAC) is provided by The Danish National Research Foundation (Grant DNRF106). BiSON is funded by the Science and Technology Facilities Council (STFC). We thank the anonymous reviewers for their help and useful comments.

APPENDIX

A. DETAILS ON BISON OBSERVATIONS AND LINE-OF-SIGHT VELOCITY EFFECTS

The BiSON solar spectrometers precisely measure the line-of-sight velocity of the solar surface by looking at the Doppler shift of a Fraunhofer line using a potassium vapour reference-cell.

The line-of-sight velocity is dominated by three components: the rotation of the Earth, the orbital velocity of the Earth, and the gravitational red-shift. At high air-masses the extended source of the Sun also suffers differential extinction which causes the line-of-sight velocity due to solar rotation to become unequally weighted across the solar disc (Davies et al. 2014). In addition to these factors are small oscillations of the solar surface which are the primary science output of the instrument, but for this analysis can be considered to be insignificant. The lab-frame absorption line is Zeeman-split by placing the vapour-cell in a longitudinal magnetic field which, when combined with suitable polarisation control, places the passbands of the spectrometer on the wings of the corresponding solar absorption-line at the points that provide the highest sensitivity to Doppler-shift caused by the line-of-sight velocity. By taking the sum of the intensity measured on both wings of the absorption line, this can be used as a proxy for the total intensity. If the solar absorption line is modelled as a thermally and rotationally broadened Gaussian, then the left panel of Figure 10 shows the expected scattered-sum of the two wings when the Doppler-velocity is zero, and for when the Doppler-velocity is at the maximum expected red-shift of 1600 ms^{-1} . Neither scattered-sum correctly recovers the unity-intensity continuum outside the Gaussian that would be measured from the transmitted light.

The difference between the measurement of the transmitted light and the scattered-sum varies with Doppler-velocity. The right panel of Figure 10 shows the expected effect of this in the absence of atmospheric extinction over the range of line-of-sight velocities experienced during a typical day. The amplitude of the daily change in effective-intensity

Table 3. Summer extinction coefficients from all sites. In the northern hemisphere the measured summer months each year are the beginning of July to the end of August, and in the southern hemisphere the beginning of January until the end of the February. Only 1995 onwards has been considered in order to remove any exceptional atmospheric events. The data-sets are sufficiently large that the standard error of the mean (i.e., σ/\sqrt{N}) is very small and therefore not presented.

Location	Detector	Mode	Median	Mean	Sigma
Mount Wilson	Transmission (Morning)	0.053	0.077	0.084	0.041
Mount Wilson	Transmission (Afternoon)	0.050	0.082	0.095	0.062
Mount Wilson	Scatter (Morning)	0.053	0.057	0.065	0.031
Mount Wilson	Scatter (Afternoon)	0.037	0.076	0.088	0.056
Las Campanas	Transmission (Morning)				
Las Campanas	Transmission (Afternoon)				
Las Campanas	Scatter (Morning)	0.032	0.042	0.046	0.017
Las Campanas	Scatter (Afternoon)	0.040	0.041	0.044	0.016
Izaña	Transmission (Morning)	0.057	0.073	0.151	0.133
Izaña	Transmission (Afternoon)	0.057	0.075	0.147	0.136
Izaña	Scatter (Morning)	0.048	0.070	0.142	0.130
Izaña	Scatter (Afternoon)	0.047	0.070	0.141	0.135
Sutherland	Transmission (Morning)	0.043	0.046	0.050	0.022
Sutherland	Transmission (Afternoon)	0.044	0.046	0.048	0.013
Sutherland	Scatter (Morning)	0.036	0.040	0.044	0.021
Sutherland	Scatter (Afternoon)	0.037	0.040	0.042	0.014
Carnarvon	Transmission (Morning)	0.085	0.100	0.115	0.078
Carnarvon	Transmission (Afternoon)	0.095	0.107	0.114	0.045
Carnarvon	Scatter (Morning)	0.119	0.106	0.119	0.068
Carnarvon	Scatter (Afternoon)	0.081	0.103	0.110	0.046
Narrabri	Transmission (Morning)	0.076	0.074	0.081	0.030
Narrabri	Transmission (Afternoon)	0.073	0.077	0.086	0.041
Narrabri	Scatter (Morning)	0.060	0.068	0.074	0.026
Narrabri	Scatter (Afternoon)	0.060	0.061	0.068	0.035

Table 4. Winter extinction coefficients from all sites. In the northern hemisphere the measured winter months each year are the beginning of January until the end of the February, and in the southern hemisphere the beginning of July to the end of August. Only 1995 onwards has been considered in order to remove any exceptional atmospheric events. The data-sets are sufficiently large that the standard error of the mean (i.e., σ/\sqrt{N}) is very small and therefore not presented.

Location	Detector	Mode	Median	Mean	Sigma
Mount Wilson	Transmission (Morning)	0.048	0.077	0.086	0.051
Mount Wilson	Transmission (Afternoon)	0.075	0.070	0.074	0.032
Mount Wilson	Scatter (Morning)	0.046	0.060	0.070	0.035
Mount Wilson	Scatter (Afternoon)	0.053	0.056	0.059	0.027
Las Campanas	Transmission (Morning)				
Las Campanas	Transmission (Afternoon)				
Las Campanas	Scatter (Morning)	0.028	0.028	0.031	0.015
Las Campanas	Scatter (Afternoon)	0.027	0.028	0.030	0.010
Izaña	Transmission (Morning)	0.045	0.048	0.059	0.035
Izaña	Transmission (Afternoon)	0.045	0.048	0.062	0.062
Izaña	Scatter (Morning)	0.042	0.043	0.051	0.030
Izaña	Scatter (Afternoon)	0.038	0.038	0.047	0.045
Sutherland	Transmission (Morning)	0.038	0.049	0.061	0.042
Sutherland	Transmission (Afternoon)	0.039	0.044	0.056	0.046
Sutherland	Scatter (Morning)	0.033	0.041	0.057	0.056
Sutherland	Scatter (Afternoon)	0.029	0.037	0.049	0.045
Carnarvon	Transmission (Morning)	0.051	0.056	0.065	0.028
Carnarvon	Transmission (Afternoon)	0.056	0.060	0.065	0.026
Carnarvon	Scatter (Morning)	0.051	0.060	0.068	0.032
Carnarvon	Scatter (Afternoon)	0.052	0.053	0.059	0.026
Narrabri	Transmission (Morning)	0.057	0.058	0.061	0.024
Narrabri	Transmission (Afternoon)	0.064	0.061	0.064	0.016
Narrabri	Scatter (Morning)	0.040	0.046	0.050	0.017
Narrabri	Scatter (Afternoon)	0.044	0.046	0.049	0.016

varies throughout the year with changes in Earth's orbital velocity, and this creates a very small seasonal effect in the scattering extinction coefficients. The increased effective-intensity is most pronounced at high red-shifts experienced during the local-afternoon of each site. The gradual increase in effective-intensity will cause any extinction coefficients derived from the scattered-sum to have a slight over-estimate in the morning and a larger under-estimate in the afternoon.

If the precise shape and depth of the solar absorption-line were known, then it would be possible to correct for this effect and recover the equivalent transmitted-intensity. Unfortunately the solar disc-integrated line profile changes with magnetic activity and so one can not correct based on a single line profile. Barreto et al. (2014) have resolved this problem for our data from Izaña by making use of a quasi-continuous Langley calibration technique, where they have achieved a *mean bias* (defined as the mean difference between the transmission and scattering extinction coefficients) of ≤ 0.01 .

In practice, extinction data from the scattering detectors offers a slight under-estimate of extinction in comparison to transmitted measurements for both morning and afternoon periods. However, this is simply a small systematic offset on the absolute value, and the extinction coefficients observed from real data are otherwise identical to those derived from the transmitted light and show the same trends.

REFERENCES

- Barreto, A., Cuevas, E., Pallé, P., et al. 2014, Atmospheric Measurement Techniques, 7, 4103
- Davies, G. R., Chaplin, W. J., Elsworth, Y., & Hale, S. J. 2014, Monthly Notices of the Royal Astronomical Society, 441, 3009. <http://dx.doi.org/10.1093/mnras/stu803>
- Fischer, G., Hill, F., Jones, W., et al. 1986, SoPh, 103, 33
- García-Gil, A., Muñoz-Tuñón, C., & Varela, A. M. 2010, Publications of the Astronomical Society of the Pacific, 122, 1109. <http://stacks.iop.org/1538-3873/122/i=895/a=1109>
- Guerrero, M. A., García-López, R. J., Corradi, R. L. M., et al. 1998, NewAR, 42, 529
- Hale, S. J. 2017, BiSON - Atmospheric extinction coefficients in the I_c band - 1984 to 2016, University of Birmingham, UK: Birmingham Solar Oscillations Network. <http://epapers.bham.ac.uk/3022/>
- Hale, S. J., Howe, R., Chaplin, W. J., Davies, G. R., & Elsworth, Y. P. 2016, Solar Physics, 291, 1. <http://dx.doi.org/10.1007/s11207-015-0810-0>
- Hill, F., Fischer, G., Forgach, S., et al. 1994, SoPh, 152, 351
- Jimenez, A., Gonzalez Jorge, H., & Rabello-Soares, M. C. 1998, A&AS, 129, 413
- Kasten, F., & Young, A. T. 1989, Appl. Opt., 28, 4735. <http://ao.osa.org/abstract.cfm?URI=ao-28-22-4735>
- Kilkenny, D. 1995, The Observatory, 115, 25
- King, D. L. 1985, Atmospheric Extinction at the Roque de los Muchachos Observatory, La Palma, RGO/La Palma Technical Note 31, Instituto de Astrofísica de Canarias, La Laguna, Tenerife, Canary Islands. http://www.ing.iac.es/Astronomy/observing/manuals/ps/tech_notes/tn031.pdf
- Laken, B. A., Parviainen, H., García-Gil, A., et al. 2016, Journal of Climate, 29, 227
- Laken, B. A., Parviainen, H., Pallé, E., & Shahbaz, T. 2014, Quarterly Journal of the Royal Meteorological Society, 140, 1058. <http://dx.doi.org/10.1002/qj.2170>
- Roca Cortés, T., & Pallé, P. L. 2014, MNRAS, 443, 1837
- Siher, E., Benkhaldoun, Z., & Fossat, E. 2002, Experimental Astronomy, 13, 159. <http://dx.doi.org/10.1023/A:1025535615069>
- Siher, E. A., Ortolani, S., Sarazin, M. S., & Benkhaldoun, Z. 2004, in Proc. SPIE, Vol. 5489, Ground-based Telescopes, ed. J. M. Oschmann, Jr., 138–145